Acta Crystallographica Section F
Structural Biology and Crystallization Communications
ISSN 1744-3091

Expression, purification, crystallization and preliminary X-ray analysis of ORF60, the small subunit (R2) of ribonucleotide reductase from Kaposi's sarcoma-associated herpesvirus (KSHV)

Daniel Gurmu,[a,b] Sue-Li Dahlroth,[a,b] Juergen Haas,[c,d] Pär Nordlund[a]* and Heidi Erlandsen[e]*

[a]Medical Biochemistry and Biophysics, Karolinska Institutet, Scheeles Väg 2, SE-171 77 Stockholm, Sweden, [b]Department of Biochemistry and Biophysics, Arrhenius Laboratories for Natural Sciences, Stockholm University, SE-106 91 Stockholm, Sweden, [c]Max von Pettenkofer Institut, Ludvig Maximillian Universität, Pettenkoferstrasse 9a, D-80336 München, Germany, [d]Division of Pathway Medicine, University of Edinburgh, 49 Little France Crescent, Edinburgh EH16 4SB, Scotland, and [e]University of Alabama at Birmingham, School of Dentistry, Institute of Oral Health Research, 1919 7th Avenue South, Birmingham, Alabama 35294, USA

Correspondence e-mail: par.nordlund@ki.se, herlands@uab.edu

Received 25 January 2010
Accepted 30 April 2010

Ribonucleotide reductase (RNR) is responsible for converting ribonucleotides to deoxyribonucleotides, which are the building blocks of DNA. The enzyme is present in all life forms as well as in some large DNA viruses such as herpesviruses. The α-herpesviruses and γ-herpesviruses encode two class Ia RNR subunits, R1 and R2, while the β-herpesvirus subfamily only encode an inactive R1 subunit. Here, the crystallization of the R2 subunit of RNR encoded by the ORF60 gene from the oncovirus Kaposi's sarcoma-associated γ-herpesvirus (KSHV) is reported. These are the first crystals of a viral R2 subunit; the use of *in situ* proteolysis with chymotrypsin and the addition of hexamine cobalt(III) chloride that were necessary to obtain crystals are described. Optimization of the crystallization conditions yielded crystals that diffracted to 2.0 Å resolution. The crystals belonged to space group $P2_1$, with unit-cell parameters $a = 63.9$, $b = 71.2$, $c = 71.8$ Å, $\alpha = 90$, $\beta = 106.7$, $\gamma = 90^\circ$. The data set collected was 95.3% complete, with an $R_{\rm merge}$ of 9.6%. There are two molecules in the asymmetric unit, corresponding to a solvent content of 43.4%.

1. Introduction

The enzyme ribonucleotide reductase (RNR) is present in all life forms as well as in some large DNA viruses such as herpesviruses (Eklund *et al.*, 2001). This allosterically regulated enzyme is responsible for the reduction of all four ribonucleotides to their corresponding deoxyribonucleotides (dNTPs), which are the building blocks of DNA. This reaction involves a free radical (Eklund *et al.*, 2001) and the activity of RNR regulates the cellular levels of the dNTP pool, ensuring that precise DNA replication and repair occurs. Based on the source of the radical cofactor used in the reductive reaction, RNRs have been divided into three classes: I, II and III. Class I is further divided into subclasses Ia and Ib. Class I RNRs are composed of a heterotetramer, which is in turn composed of two homodimers of the R1 and R2 subunits. The R1 subunit contains the active site as well as the sites for allosteric regulation. The R2 subunit contains a di-iron site, which generates a free radical by the reductive cleavage of molecular oxygen. The free radical is subsequently transferred to the R1 subunit, activating the nucleotide substrate for catalysis. In eukaryotes the activity of the RNR enzyme is cell-cycle dependent and reaches its highest level during the S phase, when DNA synthesis and replication occur (Nordlund & Reichard, 2006). The regulation of the R2 subunit takes place on a transcriptional level as well as by protein degradation and this regulation is rate-limiting for the activity of the RNR holoenzyme. The R2 gene is normally not transcribed in resting cells. However, certain events, such as DNA repair and synthesis of mitochondrial DNA, require that the synthesis of deoxyribonucleotides also occurs in resting cells. Thus, in order to synthesize dNTPs in response to DNA damage, quiescent cells are able to synthesize another cellular R2, p53R2, which may form a functional enzyme together with cellular R1 (Eklund *et al.*, 2001; Nordlund & Reichard, 2006). Its name reflects the fact that it is controlled/regulated by the transcription factor and the tumour suppressor p53. In addition, viral replication in infected cells may also trigger the production of dNTPs.

Herpesviruses represent one of the best characterized members of the large family of DNA viruses that are known to cause disease in

humans as well as in other vertebrates (Boehmer & Nimonkar, 2003). Members of the *Herpesviridae* family include human pathogens such as herpes simplex virus, varicella zoster virus, cytomegalovirus, Epstein–Barr virus (EBV) and Kaposi's sarcoma-associated herpesvirus (KSHV). Owing to differences in genomic content, organization and cellular tropism, mammalian herpesviruses may be classified as belonging to one of three subfamilies: the α-, β- and γ-subfamilies (Lembo & Brune, 2009). Interestingly, the members of the α- and γ-subfamilies encode two class Ia subunits (R1 and R2) of the RNR enzyme, while the β-herpesviruses encodes an inactive R1 subunit (Lembo & Brune, 2009). The presence of a fully functional RNR in the α- and γ-subfamilies, despite the host already encoding a functional enzyme of its own, indicates that the virus may have evolved to ensure a sufficient supply of nucleotides even if the host is in a quiescent state. The oncovirus KSHV, together with EBV, belongs to the γ-subfamily of human herpesviruses. The R2 subunit of herpesviruses, encoded by the ORF60 gene in KSHV, shares low sequence identity to other R2s of bacterial and eukaryotic origin (Nordlund & Reichard, 2006). To date, no structure of an R2 subunit from a herpesvirus has been published. An interesting feature of the amino-acid sequence is that a glutamate, Glu64, is found in the position that is usually occupied by a metal-coordinating aspartate in other R2s. Structural studies of this enzyme are important as the protein will serve as a potential drug target for the treatment of herpesviral infections and associated forms of cancer. Here, the crystallization of the R2 subunit, encoded by the ORF60 gene, from KSHV using an *in situ* proteolysis approach is described. This approach was essential in obtaining diffraction-grade crystals.

2. Materials and methods

2.1. Cloning, expression and purification

The ORF60 gene encoding residues 1–305 was cloned as described previously (Uetz *et al.*, 2006) and subsequently subcloned using the Gateway system (Invitrogen, Carlsbad, California, USA) into the pTH27 expression vector (Hammarström *et al.*, 2006). The vector encodes a polypeptide consisting of the ORF60 protein with an N-terminal extension (MGPHHHHHHLESTSLYKKAGS). This N-terminal extension encompasses an *att*B1 site for the Gateway recombination event and a His tag to facilitate protein purification (Hammarström *et al.*, 2006).

The ORF60 protein was overexpressed in *Escherichia coli* BL21 (DE3) cells (Stratagene, Cedar Creek, Texas, USA). A single colony was used to inoculate an overnight culture of 30 ml Luria–Bertani (LB) medium containing 50 µg ml^{-1} carbenicillin. 10 ml of the overnight culture was subsequently added to a larger volume (1 l) of Terrific Broth (TB) medium supplemented with 50 µg ml^{-1} carbenicillin. The cells were grown at 310 K until an $OD_{600\,nm}$ of approximately 1.0 was reached. At this point, the temperature was reduced to 291 K and ORF60 protein expression was induced by the addition of isopropyl β-D-1-thiogalactopyranoside (IPTG) to a final concentration of 0.1 m*M* and left overnight in the shaker-incubator. The cells were then harvested by centrifugation and the pellet was resuspended in lysis buffer [50 m*M* sodium phosphate pH 8.0, 500 m*M* NaCl, 10%(*v*/*v*) glycerol, 10 m*M* imidazole pH 8.0, 10 U ml^{-1} DNaseI (Roche), 0.08 mg ml^{-1} lysozyme, one tablet of Complete EDTA-free Protease Inhibitor cocktail (Roche) per 50 ml and 0.5 m*M* TCEP] before being frozen at 253 K. For purification, the frozen cell resuspension was thawed and sonicated. The cell lysate was then centrifuged at 50 000*g* for 40 min and the supernatant was subsequently passed through a 0.22 µm filter to remove cell debris. Purification of the ORF60 protein was carried out on an ÄKTA Xpress system (GE Healthcare, Uppsala, Sweden) using immobilized metal-affinity chromatography (IMAC) and gel filtration. The crude extract was loaded onto a 5 ml HisTrap FF column (GE Healthcare) pre-equilibrated in buffer 1 [50 m*M* sodium phosphate pH 8.0, 500 m*M* NaCl, 10%(*v*/*v*) glycerol, 10 m*M* imidazole pH 8.0 and 0.5 m*M* TCEP]. In addition to washing with buffer 1, a second wash was performed using buffer 1 with 70 m*M* imidazole pH 8.0. ORF60 was then eluted with elution buffer [the same as buffer 1 but with 500 m*M* imidazole pH 8.0 and one tablet of Complete EDTA-free Protease Inhibitor (Roche) per 50 ml]. The fractions that contained the protein of interest from the IMAC elution were pooled prior to loading onto

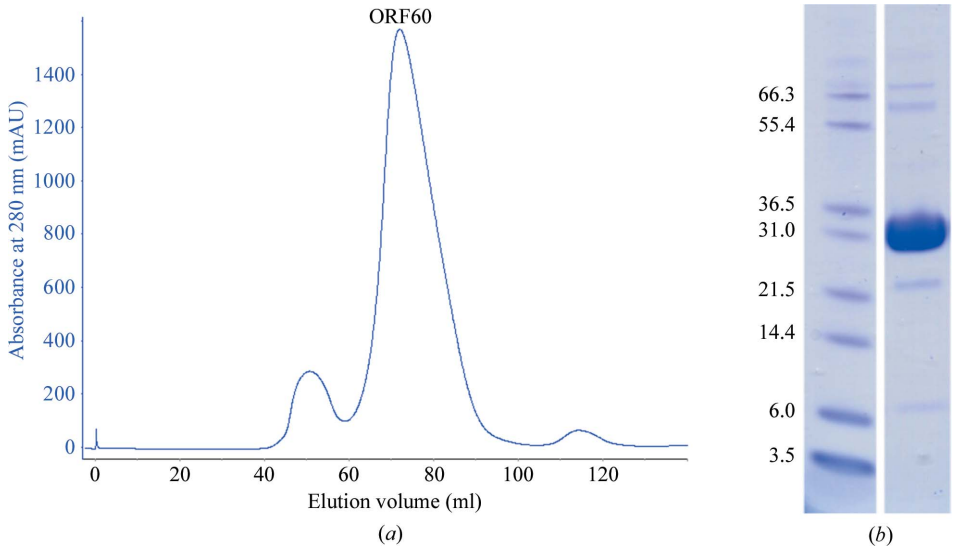

Figure 1
(*a*) Gel-filtration chromatogram of ORF60 eluted from a HiLoad 26/60 Superdex 200 gel-filtration column. The fractions corresponding to the major peak (ORF60) were pooled and concentrated and used in crystallization experiments. (*b*) Coomassie-stained SDS–PAGE (4–12%) gel of ORF60 protein eluted from the gel-filtration column, showing the typical purity of the protein sample used for crystallization experiments. The left lane contains protein molecular-weight markers (kDa). The ORF60 protein elutes at a approximate molecular weight of 31 kDa; however, mass spectrometry confirmed the exact molecular weight based on the full-length construct to be closer to 37 kDa.

Table 1
Data-collection and processing statistics.

Values in parentheses are for the highest resolution shell.

Beamline	ID29, ESRF
Wavelength (Å)	0.976
Space group	$P2_1$
Unit-cell parameters (Å, °)	a = 63.9, b = 71.2, c = 71.8, α = 90, β = 106.7, γ = 90
Resolution range (Å)	71.25–2.00 (2.11–2.00)
Unique observations	39715 (5268)
Redundancy	2.4 (1.9)
Completeness (%)	95.3 (87.2)
$R_{\rm merge}$† (%)	0.096 (0.616)
$\langle I/\sigma(I)\rangle$	5.9 (2.2)
Matthews coefficient $V_{\rm M}$ (Å^3 Da^{-1})	2.17
Molecules in the asymmetric unit	2
Solvent content (%)	43.4

† $R_{\rm merge} = \sum_{hkl}\sum_i |I_i(hkl) - \langle I(hkl)\rangle| / \sum_{hkl}\sum_i I_i(hkl)$, where $I_i(hkl)$ is the intensity of reflection hkl and $\langle I(hkl)\rangle$ is the mean intensity of reflection hkl.

a HiLoad 26/60 Superdex 200 gel-filtration column (GE Healthcare) pre-equilibrated in gel-filtration buffer [20 m*M* HEPES pH 7.5, 300 m*M* NaCl, 10%(*v*/*v*) glycerol and 0.5 m*M* TCEP]. The fractions that contained the ORF60 protein (Fig. 1*a*) were pooled and concentrated using an Amicon Ultra centrifugal filter device (Millipore, Bedford) with a 10 kDa molecular-weight cutoff. The purity of the protein was investigated by SDS–PAGE (Fig. 1*b*) and its molecular mass of 37 442.98 Da was verified by mass spectrometry. The protein appeared on the SDS–PAGE gel as a monomer of ∼31 kDa. The reason for the discrepancy in the molecular weight between the mass spectrum and the SDS–PAGE experiments is currently unknown. The protein concentration was determined by UV absorption at 280 nm using a spectrophotometer, based on the theoretically calculated absorption molar coefficient of 36 120 M^{-1} cm^{-1}.

2.2. Crystallization

Preliminary crystallization attempts using the sitting-drop vapour-diffusion technique were performed at 277 and 293 K with the ORF60 protein at a concentration of 10 mg ml^{-1} (in gel-filtration buffer; 20 m*M* HEPES pH 7.5, 300 m*M* NaCl, 10% glycerol). Initial crystallization screening was conducted using a Phoenix crystallization robot (Art Robbins Instruments, Sunnyvale, California, USA). 200 nl drops (100 nl protein solution mixed with 100 nl reservoir solution) were equilibrated against a reservoir that contained a larger volume (70 µl) of screening solution. Four screens from Qiagen set up at two different temperatures (277 and 293 K) were used for initial screening: Classics Suite, JCSG+ Suite, PEGs Suite and PEGs II Suite. However, these 288 different conditions did not yield any crystal hits. Therefore, *in situ* proteolysis (Dong *et al.*, 2007) was undertaken in an attempt to promote crystal formation. Chymotrypsin was mixed with the ORF60 protein to a final concentration of 0.1 mg ml^{-1} immediately before the crystallization-drop setups were repeated with the JCSG+ screen. After 2 d, we obtained crystal rods (Fig. 2*a*) in 0.2 *M* $MgCl_2$, 0.1 *M* Tris–HCl pH 8.5 and 20%(*w*/*v*) PEG 8000. However, optimization around this condition failed to produce thicker crystals that were suitable for detailed structural determination. The crystal rods only diffracted to ∼3.8 Å resolution (Fig. 2*a*). Using Additive Screen (Hampton Research, Aliso Viejo, California, USA), we identified 0.1 *M* hexamine cobalt(III) chloride {$[Co(NH_3)_6]Cl_3$} as an additive that induced the formation of thicker crystals (Fig. 2*b*). Further optimization using the hanging-drop vapour-diffusion method produced three-dimensional crystals after 2 d that diffracted to 2.0 Å resolution. The optimized reservoir solution contained 14%(*w*/*v*) PEG 8000, 0.2 *M* $MgCl_2$, 0.1 *M* Tris–HCl pH 8.2. In addition to 20 m*M* HEPES pH 7.5, 300 m*M* NaCl and 10% glycerol, the protein solution contained 0.1 mg ml^{-1} chymotrypsin and 0.1 *M* hexamine cobalt(III) chloride.

2.3. X-ray data collection and processing

Crystals were cryoprotected for 1–2 s in 20–25%(*v*/*v*) glycerol in 14%(*w*/*v*) PEG 8000, 0.2 *M* $MgCl_2$, 0.1 *M* Tris–HCl pH 8.2 prior to cryocooling in liquid nitrogen. X-ray diffraction data were collected at 100 K from a single ORF60 crystal at a wavelength of 0.97 Å on ID29 at the ESRF, Grenoble, France using an ADSC Q315R CCD detector. The crystal-to-detector distance was 313 mm and an oscillation range of 0.6° was used, resulting in the collection of a total of 200 images. The diffraction data were processed and scaled using *MOSFLM* (Leslie, 1992) and *SCALA* (Evans, 1993) from the *CCP*4 suite of programs (Collaborative Computational Project, Number 4, 1994). The space group was determined to be $P2_1$, with unit-cell

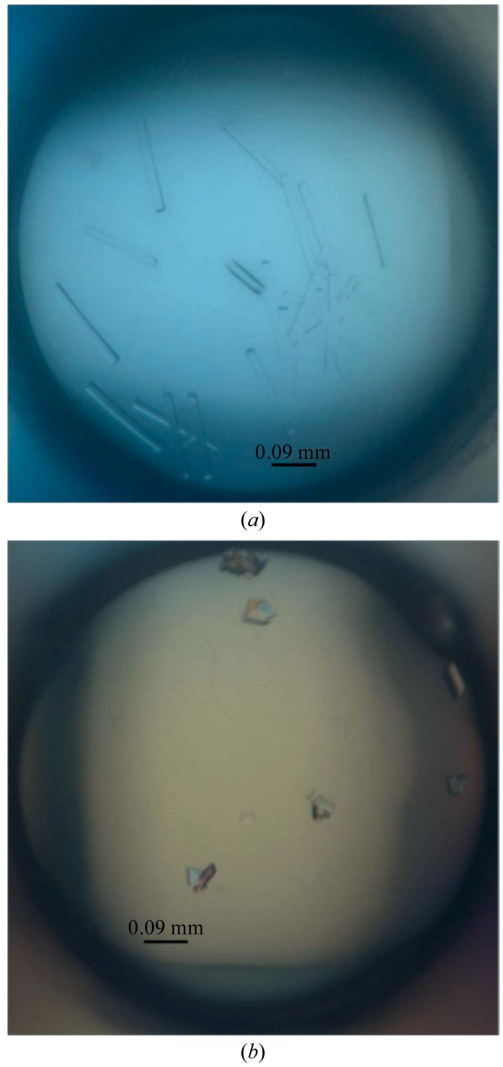

Figure 2
Crystals of ORF60 from KSHV. (*a*) Crystal rods that grew after *in situ* proteolysis with chymotrypsin. The crystal dimensions are approximately 0.18 × 0.02 × 0.02 mm. (*b*) Addition of hexamine cobalt(III) chloride to the crystallization drop resulted in the formation of thicker better diffracting crystals (2.0 Å). The crystals are presumably a truncated form of ORF60 that was produced after proteolytic cleavage by chymotrypsin. The crystal dimensions are approximately 0.7 × 0.05 × 0.02 mm.

parameters $a = 63.91$, $b = 71.20$, $c = 71.81$ Å, $\alpha = 90$, $\beta = 106.7$, $\gamma = 90^\circ$. The data-collection statistics are summarized in Table 1.

3. Results and discussion

In this paper, we report the successful expression, purification and crystallization of the first viral RNR R2 subunit (ORF60) from the Kaposi's sarcoma-associated herpesvirus. We collected high-resolution X-ray diffraction data to 2.0 Å resolution from crystals that were obtained after *in situ* proteolytic treatment of the ORF60 protein (Dong *et al.*, 2007). We believe that the *in situ* proteolysis with chymotrypsin was responsible for obtaining a crystallizable truncation of ORF60, since the 288 crystallization trials set up at two different temperatures without chymotrypsin failed to produce any crystal hits. However, structure determination of ORF60 will be necessary to confirm this. The crystals obtained by chymotrypsin treatment belonged to space group $P2_1$, with unit-cell parameters $a = 63.91$, $b = 71.20$, $c = 71.81$ Å, $\alpha = 90$, $\beta = 106.7$, $\gamma = 90^\circ$. The data set is 95.3% complete, with an $R_{\rm merge}$ of 9.6%. Computations based on the protein molecular weight indicate the presence of two molecules in the asymmetric unit, corresponding to a Matthews coefficient (Matthews, 1968) $V_{\rm M}$ of 2.17 Å^3 Da^{-1} and a calculated solvent content of 43.4%. These values are within the expected range for typical protein crystals. Further attempts to determine the structure of ORF60 by molecular replacement are currently under way using search models that show the highest sequence identity to ORF60 according to the RCSB search option: PDB codes 1jk0 (27% sequence identity; Voegtli *et al.*, 2001), 3hf1 (26% sequence identity; Smith *et al.*, 2009), 2vux (26% sequence identity; M. Welin *et al.*, unpublished work) and 1h0n (26% sequence identity; Strand *et al.*, 2002). The ORF60 structure may be of great value in the pursuit of potential drug targets for the treatment of herpesviral infections and associated forms of cancer.

References

Boehmer, P. E. & Nimonkar, A. V. (2003). *IUBMB Life*, **55**, 13–22.

Collaborative Computational Project, Number 4 (1994). *Acta Cryst.* D**50**, 760–763.

Dong, A. *et al.* (2007). *Nature Methods*, **4**, 1019–1021.

Eklund, H., Uhlin, U., Farnegardh, M., Logan, D. T. & Nordlund, P. (2001). *Prog. Biophys. Mol. Biol.* **77**, 177–268.

Evans, P. R. (1993). *Proceedings of the CCP4 Study Weekend. Data Collection and Processing*, edited by L. Sawyer, N. Isaacs & S. Bailey, pp. 114–122. Warrington: Daresbury Laboratory.

Hammarström, M., Woestenenk, E. A., Hellgren, N., Härd, T. & Berglund, H. (2006). *J. Struct. Funct. Genomics*, **7**, 1–14.

Lembo, D. & Brune, W. (2009). *Trends Biochem. Sci.* **34**, 25–32.

Leslie, A. G. W. (1992). *Jnt CCP4/ESF–EACBM Newsl. Protein Crystallogr.* **26**.

Matthews, B. W. (1968). *J. Mol. Biol.* **33**, 491–497.

Nordlund, P. & Reichard, P. (2006). *Annu. Rev. Biochem.* **75**, 681–706.

Smith, P., Zhou, B., Ho, N., Yuan, Y.-C., Su, L., Tsai, S.-C. & Yen, Y. (2009). *Biochemistry*, **48**, 11134–11141.

Strand, K. R., Karlsen, S. & Andersson, K. K. (2002). *J. Biol. Chem.* **277**, 34229–34238.

Uetz, P., Dong, Y.-A., Zeretzke, C., Atzler, C., Baiker, A., Berger, B., Rajagopala, S. V., Roupelieva, M., Rose, D., Fossum, E. & Haas, J. (2006). *Science*, **311**, 239–242.

Voegtli, W. C., Ge, J., Perlstein, D. L., Stubbe, J. & Rosenzweig, A. C. (2001). *Proc. Natl Acad. Sci. USA*, **98**, 10073–10078.